^{1}H NMR Study of the Solution Properties of the Polypeptide Neurotoxin I from the Sea Anemone *Stichodactyla helianthus*†

Raymond S. Norton,*,‡ Anne I. Cossins,‡ and William R. Kem§

School of Biochemistry, University of New South Wales, Kensington, New South Wales 2033, Australia, and Department of Pharmacology and Therapeutics, University of Florida, Gainesville, Florida 32610

Received August 4, 1988; Revised Manuscript Received September 21, 1988

ABSTRACT: The solution properties of the polypeptide neurotoxin I from the sea anemone *Stichodactyla helianthus* (Sh I) have been investigated by high-resolution ^{1}H nuclear magnetic resonance (NMR) spectroscopy at 300 MHz. The pH dependence of the spectra has been examined over the range 1.1–12.2 at 27 °C. Individual pK_a values have been obtained for the α-ammonium group of Ala-1 (8.6) and the side chains of Glu-8 (3.7), Tyr-36 (10.9), and Tyr-37 (10.8). For the remaining seven carboxyl groups in the molecule (from five Asp, Glu-31, and the C-terminus), four pK_a values, viz., 2.8, 3.5, 4.1 and 6.4, can be clearly identified. The five Lys residues titrate in the range 10.5–11, but individual pK_a values could not be obtained because of peak overlap. Conformational changes associated with the protonation of carboxylates occur below pH 4, while in the alkaline pH range major unfolding occurs above pH 10. The molecule also unfolds at elevated temperatures, having a transition temperature of ca. 55 °C at pH 5.25. Exchange of the backbone amide protons has been monitored at various values of pH and temperature in the ranges pH 4–5 and 12–27 °C. Up to 18 slowly exchanging amides are observed, consistent with the existence of a core of hydrogen-bonded secondary structure, most probably β-sheet. Comparison of these properties of Sh I in solution with those of the related polypeptides anthopleurin A and *Anemonia sulcata* toxins I and II indicates that Sh I is less stable thermally and that there are some significant differences in the ionic interactions that maintain the tertiary structure. The solvent accessibility of aromatic residues has been probed with photochemically induced dynamic nuclear polarization NMR at 360 MHz. The aromatic rings of Trp-30 and both Tyr residues are accessible to flavin dye, but Tyr-37 shows a weaker response then Tyr-36, suggesting that Tyr-37 is partially shielded.

Sea anemones contain a series of polypeptides of $M_r \sim 5000$ that bind to the sodium channels of nerve and muscle cells, thereby prolonging the duration of the action potential in those tissues (Norton, 1981; Alsen, 1983; Kem, 1988). The best characterized of these toxins are anthopleurin A (AP-A),[1] from the northern Pacific anemone *Anthopleura xanthogrammica*, and ATX II, from the Mediterranean species *Anemonia sulcata*, which display extensive (86%) sequence homology. A number of other polypeptides from these anemones, as well as from several other species, have similar biological activities to those of AP-A and ATX II, although a broad spectrum of species and tissue specificities is observed (Schweitz et al., 1985).

AP-A and ATX II were isolated from anemones belonging to the family Actiniidae. Recently, several groups have also investigated polypeptide toxins from anemones of the family Stichodactylidae, including *Heteractis* [formerly *Radianthus* (Dunn, 1981)] *paumotensis* (Schweitz et al., 1985; Wemmer et al., 1986; Metrione et al., 1987), *Heteractis macrodactylus* (Zykova et al., 1985), and *Stichodactyla* (formerly *Stoichactis*) *helianthus* (Kem et al., 1986; Pennington et al., 1988). These toxins are similar to those from the actiniid anemones with respect to the locations of the half-cystines (and presumably therefore the disulfide bonds), as well as several other residues thought to play a role in biological activity or maintenance of the tertiary structure (see Figure 1). They differ, however, in several important respects, including the distribution of charged side chains and the sequences at the N- and C-termini. Moreover, while they have a similar effect on the sodium channel to that of the actiniid toxins and can prevent the binding of scorpion toxins to the channel, they cannot prevent binding of the actiniid toxins to the channel. Furthermore, they are immunologically distinct, showing no cross-reactivity with antibodies raised against the *A. xanthogrammica* or *A. sulcata* polypeptides (Schweitz et al., 1985).

It may be expected that the different chemical and biological properties of the stichodactylid toxins will be reflected in their structures and molecular properties in solution. Previously, we have investigated ATX I, ATX II, and AP-A by means of ^{13}C NMR (Norton & Norton, 1979; Norton et al., 1980, 1982) and ^{1}H NMR (Gooley et al., 1984a,b, 1986, 1988; Gooley & Norton, 1985, 1986a,b) spectroscopy. This has culminated in the recent determination of the backbone folding of AP-A in solution using distance geometry and restrained molecular dynamics calculations (Torda et al., 1988). In order to compare the structures and solution properties of the two classes of anemone polypeptides, we have undertaken a ^{1}H NMR study of some representative members of the stichodactylid-type toxins. In this paper we describe the pH and temperature dependence and the backbone amide exchange rates of one of these, neurotoxin I from *S. helianthus* (Sh I).

† This work was supported in part by grants from the Australian Research Grants Scheme (R.S.N.) and the National Institutes of Health (Grant GM 32848 to W.R.K).

* Address correspondence to this author.
‡ University of New South Wales.
§ University of Florida.

[1] Abbreviations: Sh I, *Stichodactyla* (formerly *Stoichactis*) *helianthus* neurotoxin I; AP-A, anthopleurin A; ATX I and II, *Anemonia sulcata* toxins I and II; 2D NMR, two-dimensional nuclear magnetic resonance; HOHAHA, homonuclear Hartmann–Hahn 2D spectroscopy; photo-CIDNP, photochemically induced dynamic nuclear polarization.

0006-2960/89/0428-1820$01.50/0

```
              5        10       15       20       25
Sh I      AACKC    DDEGP    DIRTA    PLTGT    VDLGS
AP-A      GVSCLC   DSDGP    SVRGN    TLSGT    LWLYPS

             30       35       40       45
Sh I      CNAGW    EKCAS    YYTII    ADCCR    KKK
AP-A      GCPSGW   HNCKA    HGPTI    GWCCK    Q
```

FIGURE 1: Amino acid sequences of *Stichodactyla helianthus* neurotoxin I (Kem et al., 1986) and anthopleurin A (Norton, 1981), aligned to indicate sequence homology. The residue numbering system is that of Sh I.

In the following paper in this issue (Fogh et al., 1989), sequence-specific ^{1}H resonance assignments for Sh I are presented and its ordered secondary structure is described.

Materials and Methods

Materials. Sh I was purified from *S. helianthus* collected in the Caribbean as described by Kem et al. (1986). High-performance liquid chromatographic analysis of this material on a Vydac C18 column (Gooley et al., 1988) showed that it contained several minor polypeptide impurities, the major component (Sh I) comprising 85–90%. These minor species did not interfere with interpretation of the spectral data. Labile protons were exchanged with deuterium by incubation of the protein in ^2H_2O (>99.75% ^{2}H, from the Australian Atomic Energy Commission, Lucas Heights, NSW) for up to 12 h at room temperature, followed by lyophilization. Protein concentrations for one-dimensional NMR measurements were in the range 0.8–3 mM.

NMR Spectroscopy. Most ^{1}H NMR spectra were recorded at 300.07 MHz on a Bruker CXP-300 spectrometer operating in the pulsed Fourier transform mode with quadrature detection; 5 mm o.d. spinning sample tubes (Wilmad Glass Co., 527-PP grade) were used. The probe temperature was maintained with a Bruker B-VT 1000 variable-temperature unit and calibrated by using methanol and/or ethylene glycol standards. Typical spectral accumulation parameters were as follows: sweep width 3400 Hz, 8192 points, 90° radio-frequency pulses, 2.0-s recycle time, 500–2000 accumulations, probe temperature 27 °C. Resolution enhancement was effected by a Lorentzian–Gaussian transformation, and data were zero-filled to 16 384 or 32 768 points prior to Fourier transformation. Chemical shifts were measured digitally, with 1,4-dioxane, at 3.751 ppm downfield from 2,2-dimethyl-2-silapentane-5-sulfonate (DSS) as internal standard.

Some NMR spectra in the pH series were recorded at 300.06 MHz on a Nicolet NT-300 spectrometer equipped with a 1280 computer. Spectra were run at 25 °C and processed with a double exponential for resolution enhancement.

pH Dependence. pH values were measured at 22 °C with an Activon Model 101 pH meter and Ingold 6030-02 microelectrode. Reported values are pH meter readings uncorrected for deuterium isotope effects or possible Na^+ effects at high pH. The pH was adjusted by adding ca. 0.5 M ^{2}HCl or NaO^{2}H and was measured both before and after NMR experiments. pK_a values were obtained by nonlinear least-squares fits of the observed chemical shifts to the Henderson–Hasselbalch equation for a single ionization, assuming fast exchange between the conjugate acids and bases.

Amide Proton Exchange. Four series of measurements were carried out, two at 27 °C (pH 4.03 and 5.15) and two at 12 °C (pH 4.44 and 4.91). In each case a sample of normal isotopic Sh I was dissolved in acidified ^2H_2O, the pH was adjusted if necessary, and spectral acquisition commenced within 15–30 min of dissolution. Spectra were acquired with 500–1500 transients and 2.0-s recycle time over a period of 1–2 days. The midpoint of the acquisition period of each spectrum was taken as the time for kinetic analysis.

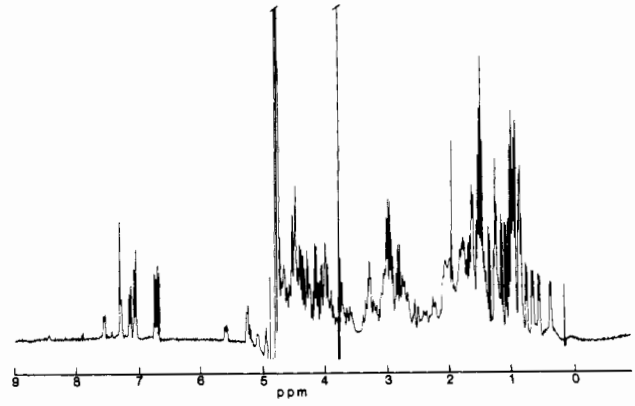

FIGURE 2: 300-MHz ^{1}H NMR spectrum of Sh I in ^2H_2O at pH 5.5 and 27 °C. The time domain data were multiplied by a Lorentz–Gauss window function and zero-filled to 16 384 data points before Fourier transformation. The dioxane and residual H^{2}HO resonances have been truncated. Sharp peaks are observed from the internal reference dioxane (3.751 ppm) and the impurities acetate (1.94 ppm) and silicon grease (0.15 ppm).

Heights of peaks from exchangeable protons were measured relative to those of a well-resolved resonance from a nonexchangeable proton (W30 H-2) so as to compensate for any effects of spectrometer drift or inhomogeneity broadening. For well-resolved resonances, peak heights were measured directly from the spectra. In some cases difference spectroscopy was used, where a spectrum acquired toward the end of the experiment was subtracted from an earlier spectrum. Decay rates were obtained by assuming first-order kinetics and using nonlinear regression to an exponential decay. Estimated errors in k_m are ±15% for data at 12 °C and ±25% for data at 27 °C (where signal-to-noise ratios were lower due to lower protein concentrations). Because of the time resolution of the experiments, the highest k_m that could be measured was on the order of 10^{-2} min^{-1}. For very slowly exchanging protons, no attempt was made to determine k_m if the peak height did not decay by at least 25% during the observation period. Instead, a conservative upper limit for k_m was estimated, on the basis of the peak not having halved in height. In most experiments this limit was on the order of 10^{-4} min^{-1}.

Photo-CIDNP. Spectra were recorded at 360 MHz on a Bruker HX-360 at the University of Groningen NMR Facility, as described previously (Kaptein, 1982; Norton et al., 1986). Laser pulses of 0.1- and 0.6-s duration were employed, and spectra were processed with 1.0-Hz exponential broadening.

Bioassay. Neurotoxic activity was assayed by intrahemocoelic injection of toxin dissolved in phosphate-buffered saline into soldier crabs *Mictyris longicarpus* (average weight 3 g). The crabs were placed on their backs, and their ability to right themselves 10 min after injection was measured. Controls were injected with comparable volumes of phosphate-buffered saline alone.

Results

Figure 2 shows the 300-MHz ^{1}H NMR spectrum of Sh I at pH 5 and 27 °C. The spectrum displays a number of upfield-shifted methyl resonances which are indicative of a folded structure (Wüthrich, 1986). There is no evidence of major conformational heterogeneity of the type encountered in AP-A and ATX II (Gooley et al., 1984b, 1988).

In the following sections the effects of pH and temperature on Sh I are investigated, and the amide exchange rates are characterized. These results also provide the basis for selection of appropriate solution conditions for 2D NMR studies di-

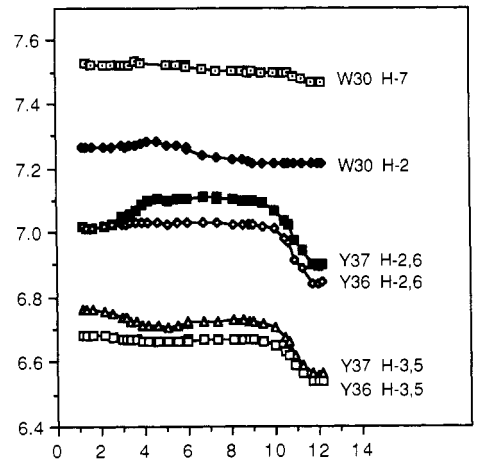

FIGURE 3: pH dependence of the chemical shifts of aromatic proton resonances of Sh I in ^2H_2O at 27 °C.

rected toward defining the structure of Sh I. The next step in this process, that of making sequence-specific resonance assignments, is described in the following paper in this issue (Fogh et al., 1989). Where appropriate, these resonance assignments are utilized in the present discussion.

Effects of pH. Sh I contains 18 ionizable groups, arising from the N- and C-termini (Ala and Lys, respectively), Glu-8 and -31, Arg-13 and -45, Tyr-36 and -37, five Asp residues (at positions 6, 7, 11, 22, and 42) and five lysines (at positions 4, 32, 46, 47, and 48). As a consequence, the pH dependence of its NMR spectrum is complex and individual pK_a values cannot be assigned to all ionizable groups.

The effects of pH on well-resolved resonances in the aromatic region of the spectrum are summarized in Figure 3. The ionizations of the phenolic groups of Tyr-36 and -37 are clearly seen. Their pK_a values are given in Table I. At pH <5 all of the resolved aromatic peaks undergo changes as carboxylate groups in the molecule become protonated. This suggests that the conformation at acid pH is different from that predominant at neutral pH, although it is difficult to link this change to the protonation of a single carboxylate because of the large number of such groups in Sh I. The titration of one of the glutamate residues, Glu-8, can be observed directly, giving a pK_a of 3.7. Other carboxyl pK_a values identifiable from the data presented in Table I are 6.4, 4.1, 3.5, and 2.8. These pK_a values cannot be assigned to individual Asp or Glu residues at this stage because of extensive peak overlap in the relevant regions of one-dimensional NMR spectra over this pH range.

The effects of the conformational change that occurs at acid pH on resonances in the methyl region of the spectrum are illustrated in Figure 4. The fact that several upfield-shifted resonances are still present at the lowest pH examined (Figure 4A) indicates that the acid-denatured form of Sh I does not behave as a random coil. Figure 4 indicates, however, that a more extensive conformational change occurs at alkaline pH. In marked contrast to the acid-denatured form, the alkaline-denatured form of Sh I shows no upfield-shifted methyl resonances (Figure 4E). In addition, the H^α resonances that occur between 5 and 6 ppm in the spectrum of native Sh I, and which are indicative of ordered secondary structure, have moved upfield at high pH. Overall, the spectrum is consistent with major unfolding of the molecule at alkaline pH. This transition is largely reversible (see below), although the chemical shifts of some resonances in the spectrum of the "renatured" form differ by up to 0.02 ppm from those in Sh I that has not been exposed to alkaline pH.

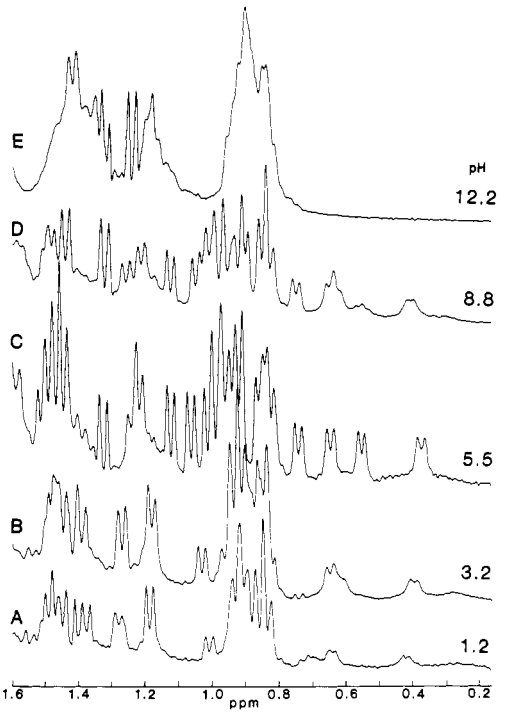

FIGURE 4: Methyl regions of 300-MHz ^1H NMR spectra of Sh I in ^2H_2O at 27 °C at the following pH values: (A) 1.2; (B) 3.2; (C) 5.5; (D) 8.8; (E) 12.2.

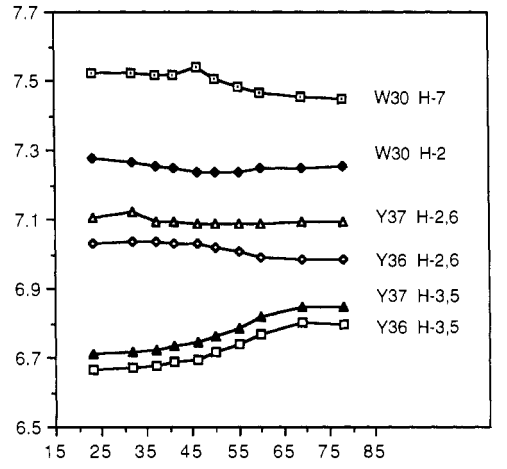

FIGURE 5: Temperature dependence of the chemical shifts of aromatic proton resonances of Sh I in ^2H_2O at pH 5.25.

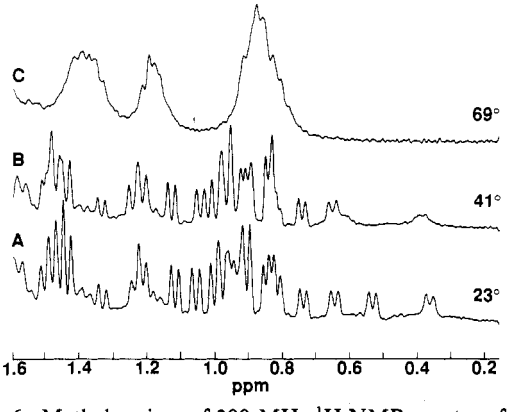

FIGURE 6: Methyl regions of 300-MHz ^1H NMR spectra of 1 mM Sh I in ^2H_2O at pH 5.25 and temperatures of (A) 23, (B) 41, and (C) 69 °C.

Effects of Temperature. Figure 5 summarizes the temperature dependence of well-resolved aromatic resonances of Sh I in ^2H_2O at pH 5.25. For comparison, the methyl regions

Table I: Titration Behavior of Residues in Sh I in ^2H_2O at 27 °C[a]

residue[b]	proton resonance	δ_A	$\delta_A - \delta_B$	pK_a (SD)
Ala-1	H_3^β	1.468	0.244	8.60 (0.14)
Glu-8	H_2^γ	2.486	0.112[c]	3.70 (0.19)
Arg-13	H_2^δ	3.220	−0.044	3.50 (0.22)
Thr-14	H_3^γ	1.187	0.064	3.61 (0.21)
Thr-18	H_3^γ	1.278	0.064	3.44 (0.19)
Val-21	H_3^γ	0.421	0.053	2.82 (0.23)
Trp-30	H-2	7.280	0.062	6.40 (0.26)
	H-7[d]	7.502	0.038	11.10 (0.30)
Tyr-36	H-2,6	7.028	0.193	10.94 (0.16)
	H-3,5[e]	6.669	0.135	10.83 (0.13)
Tyr-37	H-2,6	7.015	−0.091	3.39 (0.20)
		7.104	0.214	10.76 (0.18)
	H-3,5[f]	6.765	0.054	2.90 (0.20)
		6.728	0.175	10.78 (0.16)
Thr-38	H_3^γ	0.721	0.189	2.76 (0.14)
		0.536	−0.109	6.45 (0.20)
Ile-39	H_3^γ	0.998	−0.062	2.90 (0.23)
Ala-41	H_3^β[g]	1.276	0.043	4.14 (0.21)

[a] δ_A and δ_B are limiting chemical shifts at the acidic and basic extremes of the titration to which the pK_a refers. pK_a values were determined from nonlinear least-squares fits to the equation for a single ionization. Standard deviations are given in parentheses. pK_a values are shown only for titrations of well-resolved resonances with $|\delta_A - \delta_B| \geq 0.038$ ppm. [b] Assignments are taken from Fogh et al. (1989). [c] Average value, as the two H^γ resonances have distinct chemical shifts at pH > pK_a. [d] Trp-30 H-7 resonance moves upfield by 0.02 ppm between pH 4 and 8. [e] Tyr-36 H-3,5 doublet undergoes a 0.02 ppm upfield shift with pK_a 2.96 (0.23) and δ_A 6.683. [f] Tyr-37 H-3,5 doublet moves downfield by 0.018 ppm between pH 5 and 7. [g] Also shows inflection with pK_a 7.9 (0.45), δ_A 1.239, and δ_B 1.258.

of spectra at three different temperatures are shown in Figure 6. Two conformational transitions are apparent. The first is reflected in the H-2 resonance of Trp-30, which shifts upfield between 20 and 45 °C (Figure 5), and by changes in some of the upfield-shifted methyl resonances, most notably that of Thr-38 H_3^γ at 0.53 ppm (Figure 6). It is interesting that the Trp-30 H-2 and Thr-38 H_3^γ resonances are also affected by titration of the carboxyl group with a pK_a of 6.4, and that the directions of the shifts observed with increasing temperature over this range are the same as those observed upon ionization of this carboxyl group. The conformational change reflected by these resonances may be localized to a few residues.

At temperatures above 45 °C, Sh I undergoes major unfolding, with a transition temperature of ca. 55 °C (Figures 5 and 6). As in the case of alkaline-denatured Sh I, the heat-denatured form of the molecule has a spectrum similar to that of a random coil polypeptide (Wüthrich, 1986), with no upfield-shifted methyl peaks and no H^α resonances in the 5–6 ppm region. In both unfolding transitions (thermal and alkaline), well-resolved resonances in the spectrum of the native protein appear to be in fast or intermediate exchange with their counterparts in the denatured protein, as judged by the smooth transition of chemical shifts between values in the native and denatured forms. In both cases, unfolding also appears to be fully reversible as judged by the recovery of neurotoxic activity found after either thermal denaturation at 76 °C and pH 7 or alkaline denaturation at pH 11 and 25 °C, each for a period of 15 min.

Amide NH Exchange. Exchange of the amide protons of Sh I was investigated with one-dimensional NMR. Representative spectra from an experiment at pH 4.9 and 12 °C are shown in Figure 7. Exchange rates for the slowly exchanging amides are presented in Table II. Assignments of the slowly exchanging amide resonances were made on the basis of NH chemical shifts and confirmed by a HOHAHA spectrum recorded on normal isotopic Sh I dissolved in ^2H_2O at pH 4.9 and 12 °C (Fogh et al., 1989).

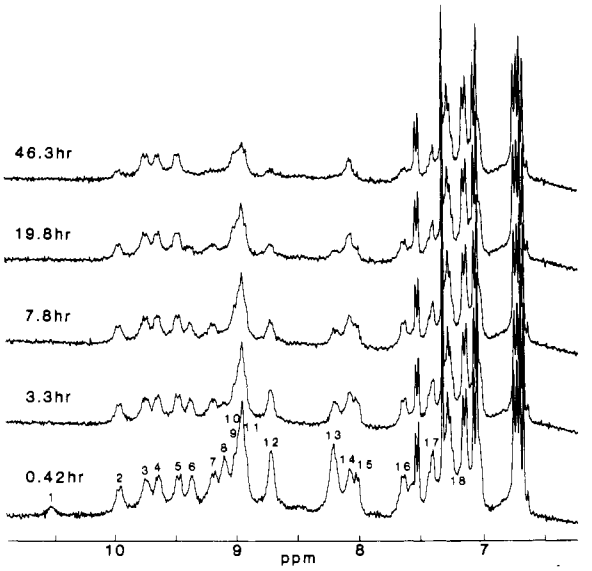

FIGURE 7: Amide NH exchange experiment on 3 mM normal isotopic Sh I dissolved in ^2H_2O at pH 4.9 and 12 °C. Times shown (in h) are the midpoints of data acquisition for each spectrum.

Table II: Chemical Shifts (ppm) and Exchange Rates (min^{-1}) of Slowly Exchanging Amide Protons of Sh I

peak[a]	δ[b]	$k_m \times 10^3$ pH 4.4, 12 °C	$k_m \times 10^3$ pH 4.9, 12 °C	$k_m \times 10^3$ pH 4.0, 27 °C	assignment[c]
1	10.54	nd[d]	>10	nd	Thr-18
2	9.99	0.5	0.4	6	Thr-20
3	9.79	<0.1	<0.1	3	Cys-33
4	9.68	<0.1	<0.1	~10	Arg-45
5	9.48	<0.1	<0.1	~10	Glu-31
6	9.39	1	1	nd	Cys-5
7	9.20	0.7	2	7	Cys-43
8	9.11	2	8	>10	Gly-24
9, 10, 11	8.96	0.7[e]	0.8[e]	2[e]	Asp-22, Trp-30, Cys-44
12	8.72	2	2	>10	Gly-19
13	8.20	1	4	>10	Asp-42
14	8.08	<0.1	0.3	2	Val-21
15	8.03	0.6	0.9	>10	Cys-3
16	7.65	0.1	0.6	5	Ala-41
17	7.40	0.7	0.3	nm[f]	Ala-34
18	7.20	nm	nm	nm	Ile-40

[a] Peak numbering corresponds to that of Figure 7. [b] Chemical shifts at pH 4.9 and 12 °C. [c] Assignments based on chemical shifts of amide resonances and confirmed by means of a HOHAHA on 6 mM Sh I at pH 4.9 and 12 °C (Fogh et al., 1989). In addition to the slowly exchanging amides, the HOHAHA spectrum also detected weak cross-peaks from the side-chain ammonium protons of Lys-46 at 7.59 to its δ- and ϵ-protons, indicating that the ammonium protons are slowly exchanging. [d] Peak exchanged too quickly for k_m to be estimated. [e] Peaks 9–11 overlap. The k_m values in this table describe the most rapidly exchanging component (from either Asp-22 or Trp-30); the other two have exchange rates $\leq 0.1 \times 10^{-3}$ min^{-1}. [f] k_m not measured because of peak overlap.

Photo-CIDNP Spectra. Figure 8 shows the aromatic region of a photo-CIDNP difference spectrum of Sh I obtained with the dye flavin I (7,8,10-trimethyl-3-(carboxymethyl)isoalloxazine). The difference spectrum contains emission peaks at 6.66 and 6.71 ppm, due to the H-3,5 doublets of Tyr-36 and Tyr-37, respectively. The intensity of the Tyr-36 emission peak is roughly twice that of the Tyr-37 peak. The only Trp residue in Sh I, Trp-30, shows strong absorption peaks at 7.03, 7.25, and 7.27 ppm, arising from H-4, H-6, and H-2, respectively (the H-6 and H-2 resonances overlap under the

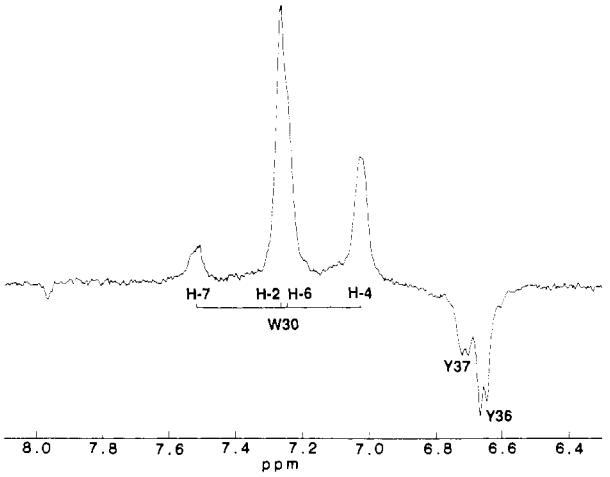

FIGURE 8: Aromatic region of photo-CIDNP difference spectrum ("light" – "dark") of Sh I in ^2H_2O at pH 5.7 recorded at 360 MHz with a 0.6-s light pulse. The "light" spectrum was acquired in one scan and the "dark" spectrum in four scans.

conditions used to acquire and process the photo-CIDNP spectra). It may be concluded that the indole ring of Trp-30 is accessible to the flavin dye (Kaptein, 1982).

A small absorption peak arising from H-7 of Trp-30 is visible in Figure 8 at 7.52 ppm. This results from polarization transfer from H-6 during the 0.6-s duration of the laser light pulse (Kaptein, 1982). The intensity of this peak relative to those of the other Trp resonances is lower in photo-CIDNP spectra recorded with a 0.1-s light pulse, where polarization transfer is less significant. The intensity of the Tyr-37 emission peak relative to that of Tyr-36 is slightly less in the 0.1-s spectrum. The remaining peak evident in Figure 8 is a small emission peak from the flavin dye at 7.97 ppm.

In the aliphatic region of the difference spectrum, absorption peaks are expected from the Tyr H^β resonances and emission peaks from the Trp H^β resonances (Kaptein, 1982). Strong emission peaks are observed at 2.94 and 3.58 ppm, in agreement with the sequence-specific assignments for the H^β resonances of Trp-30 (Fogh et al., 1989). Weak absorption peaks are present at 2.7 and 3.02 ppm, corresponding to the H^β resonances of Tyr-36.

Discussion

Several facets of the solution properties of Sh I have been investigated in this paper. In the following discussion these properties are considered both in relation to the structure of Sh I itself and in comparison with the properties of the related polypeptides AP-A, ATX I, and ATX II from actiniid anemones.

We begin by noting that Sh I shows no evidence of conformational heterogeneity in solution. This contrasts with AP-A and ATX II, which show extensive spectral heterogeneity that has been proposed to be due to cis–trans isomerism around the Gly-40 to Pro-41 peptide bond (Gooley et al., 1984b, 1988). ATX I, which lacks Pro-41, does not display conformational heterogeneity of this type (Gooley et al., 1988; Widmer et al., 1988). Sh I also lacks proline at the equivalent of position 41 in AP-A and ATX II (Figure 1), but as there is only one conserved Pro (at position 10 in Sh I), this cannot be taken as firm evidence in favor of a role for Pro-41 in the heterogeneity found in AP-A and ATX II.

The pH dependence of the spectrum of Sh I is quite complex, as expected for a polypeptide of 48 residues containing five Asp, two Glu, two Tyr, and five Lys residues, as well as free N- and C-termini. At pH >10 the molecule undergoes major unfolding to a form with a spectrum resembling that of a random coil polypeptide (Wüthrich, 1986). The ionizable groups responsible for this alkaline denaturation have not been identified, as the five lysine residues all titrate with pK_a values in the range 10.5–11.0, while Tyr-36 and -37 have phenolic pK_a values of 10.8–10.9. Only the α-ammonium moiety of Ala-1, with a pK_a of 8.6, can be eliminated from any involvement, as the structure of Sh I is still intact at pH 8.8 (Figure 4D). For both tyrosine residues the titration shifts of the H-2,6 resonances are larger than in model peptides (Bundi & Wüthrich, 1979), whereas the titration shifts of the H-3,5 resonances are smaller. These differences reflect the superposition of chemical shift changes caused by unfolding on those associated with phenolic ionization. The major unfolding of Sh I at alkaline pH stands in marked contrast to the behavior of AP-A, ATX I, and ATX II (Gooley et al., 1984a, 1988). The latter group of polypeptides show no significant conformational changes at pH values up to 13. Prolonged incubation at high pH leads to loss of activity in the case of AP-A (Norton & Norton, 1979), but this is probably a consequence of chemical changes associated with the disulfide bonds.

Differences between Sh I and the actiniid anemone polypeptides are also apparent in the acid pH range. AP-A, ATX I, and ATX II contain only three carboxyl groups, and the protonation of one of these, proposed to be Asp–9, is associated with a conformational change that affects the chemical shifts of a large number of resonances in their spectra (Gooley et al., 1988). For example, in AP-A resonances from Thr-21, Trp-23, Tyr-25, His-34, Ala-38, His-39, Trp-45, and Cys-47, as well as others for which peak overlap in one-dimensional spectra prevents pK_a measurements, are affected to varying degrees. In the spectra of Sh I a large number of resonances undergo pH-dependent changes in chemical shift below pH 4. However, while resonances from Val-21, Tyr-37, Thr-38, and Ile-39 are affected by a carboxyl group with a pK_a of 2.8,[2] resonances from another group of residues, viz., Arg-13, Thr-14, and Thr-18, are affected by a group with a pK_a of 3.5. The Leu-17 H_3^γ resonance also undergoes a significant downfield shift at pH <4.5, and although peak overlap prevents an accurate pK_a determination, this peak is probably affected by the same titration as Arg-13, Thr-14, and Thr-18. If the carboxyl group with the pK_a of 2.8 can be regarded as comparable to the structurally important carboxyl in AP-A, ATX I, and ATX II, it is clear that neither is it involved in interactions as strong as those in AP-A and ATX II, where the corresponding pK_a is about 2, nor does it play as critical a role in maintaining the tertiary structure. Another indication of this comes from the behavior of the H^α resonance of Cys-44 of Sh I at 5.6 ppm, which shifts by only about 0.03 ppm at low pH. In ATX I the corresponding resonance moves upfield by 0.1 ppm with a pK_a equivalent to that of the structurally important carboxyl (Gooley et al., 1984a), while in AP-A this peak moves upfield and broadens below pH 3 (Gooley et al., 1988). It is also noteworthy that the H_3^β resonance of Ala-41, which is separated by only one residue from Ile-39, is not affected by titration of the carboxyl with pK_a 2.8, further emphasizing the rather localized effects of its titration. It may

[2] The pK_a of 2.8 is an average of the values for Val-21 H_3^γ, Tyr-37 H-3,5, Thr-38 H_3^γ, and Ile-39 H_3^γ, weighted according to the magnitude of the respective titration shifts. Data for Tyr-37 H-2,6 were not included, as it is possible either that the chemical shifts of this resonance are affected by titration of a second carboxyl with a pK_a in the range 3.5–4, in addition to the group with a pK_a of 2.8, or that there is a nearby carboxyl with a pK_a of 3.4 (Table I).

be that the presence of a much larger number of carboxyl groups in Sh I lessens the structural role of any one individual carboxyl.

Another significant difference in Sh I concerns the identity of the carboxyl with pK_a 2.8. In ATX I the structurally important carboxylate is that of Asp-9. This is probably also true in AP-A and ATX II (Gooley et al., 1988). In Sh I, however, the equivalent residue, Glu-8, has a pK_a of 3.7 and its protonation is not responsible for any significant conformational changes. Its pK_a is slightly lower than that of glutamate residues in small peptides (Gooley et al., 1988) but not nearly as low as that of the conformationally significant carboxylate in the actiniid polypeptides. As noted above, resonances from Arg-13, Thr-14, and Thr-18 are affected by titration of a carboxyl with a pK_a of 3.5 (Table I), which could correspond to Glu-8. An equally likely candidate, however, is Asp-11, which, by analogy with AP-A (Torda et al., 1988), would be part of a large loop encompassing residues 10–17. In any case, it is clear that Glu-8 does *not* fulfill the same significant function in maintaining the overall structure as its equivalent residue, Asp-9, in the actiniid polypeptides.

The observation of a carboxyl ionization with a pK_a of 6.4 is intriguing. This has significant effects on the chemical shifts of resonances from Trp-30 and Thr-38 (Table I), as well as smaller effects on those from Tyr-37 (Table I) and some methyl groups. A possible candidate for this group is the carboxyl of Glu-31. Whichever residue it comes from, however, its pK_a is significantly higher than corresponding values in small peptides, viz., 3.9 for Asp and 4.2–4.3 for Glu (Gooley et al., 1988). Hydrogen bonding, partial screening from the solvent, or proximity to another negative charge could all contribute to the high pK_a for this carboxyl. A similar pK_a is found for Glu-35 in hen egg white lysozyme which is located in the active site cleft of that enzyme (Imoto et al., 1972). The other well-defined carboxyl pK_a in Sh I is that of 4.1, reflected by the Ala-41 H_3^β resonance (Table I). This probably represents the titration of Asp-42.

The thermal stability of Sh I is relatively low. Whereas the actiniid polypeptides do not undergo significant conformational changes even at temperatures up to 80 °C and pH values in the range 4.5–5 (Gooley et al., 1988), Sh I undergoes major unfolding with a transition temperature of about 55 °C at pH 5.25. In addition to this major transition, a more localized conformational change occurs between 20 and 45 °C. The low thermal stability of Sh I is also reflected in the exchange rates of its amide protons. Sh I has only a few amide protons with exchange rates $\leq 1 \times 10^{-3}$ min^{-1} at pH 4.0 and 27 °C, while AP-A, ATX I, and ATX II have five, seven, and nine, respectively, under similar conditions (Torda & Norton, 1987). The overall number of protons for which exchange rates could be measured is approximately the same in all four polypeptides. This is a consequence of the presence of a similar core of antiparallel β-sheet in AP-A (Gooley & Norton, 1986), ATX I (Widmer et al., 1988), and Sh I (Fogh et al., 1989). Where Sh I differs is in the reduced overall thermal stability of its tertiary structure. It has been noted previously that a correlation exists between the rates of exchange of the backbone amide protons of a protein and its thermal stability (Wagner & Wüthrich, 1978).

The photo-CIDNP experiments described in this paper provide useful information on the exposure of the three aromatic rings in Sh I. The indole ring of Trp-30 gives a strong photo-CIDNP response, indicating that it is freely accessible to the flavin dye used in these experiments. The tyrosine residues show some differences in behavior, with Tyr-37 giving a response less than half that of Tyr-36. This suggests that the phenolic ring of Tyr-37 is less exposed to the dye, and by inference the aqueous solvent, than that of Tyr-36. In selective nitration experiments using tetranitromethane, it has been found that one Tyr is less reactive than the other, although the less reactive residue has not yet been identified (W. R. Kem, unpublished results). Our results on the solvent exposure of the aromatic rings of Sh I will be useful in evaluating the final structure of the molecule generated from NMR data (R. Fogh, W. R. Kem, and R. S. Norton, unpublished results).

In conclusion, we have investigated several aspects of the solution properties of Sh I in this work and compared them with those of the related actiniid polypeptides AP-A, ATX I, and ATX II. Sh I differs in several important aspects from the actiniid polypeptides. It appears to lack a single carboxyl group which has a significantly reduced pK_a and plays a major role in stabilizing the tertiary structure. Furthermore, the carboxyl that comes closest to fulfilling this role in Sh I is not Glu-8, which is what would have been expected by analogy with AP-A, ATX I, and ATX II. At high pH, the molecule unfolds to a form with a ^{1}H NMR spectrum resembling that of a random coil. Similar unfolding occurs at high temperature. Thus, while the secondary strucutre of Sh I is very similar to those of ATX I and AP-A (Fogh et al., 1989), and the time-averaged tertiary structures are also likely to be similar, there are some significant differences in the stability of the Sh I structure to extremes of pH and temperature, in its overall flexibility as judged by amide exchange rates, and in the local ionic interactions that stabilize the structure. While the tertiary structure of a polypeptide is certainly the most important and interesting aspect of its properties in solution that can be derived from NMR data, results of the type presented here have an important role to play in providing a complete description of the behavior of the molecule in solution.

Acknowledgments

We are most grateful to Dr. Chingkuang Tu and Professor Tom Mareci for advice and assistance in acquiring spectra on the Nicolet spectrometer and to Dr. Klaas Dijkstra and Professor Robert Kaptein for access to the NMR facility in Groningen, where the photo-CIDNP experiments were carried out. We also thank Rasmus Fogh and Dr. Bridget Mabbutt for helpful discussions, particularly on resonance assignments.

Registry No. Sh I, 117860-13-6.

References

Alsen, C. (1983) *Fed. Proc., Fed. Am. Soc. Exp. Biol. 42*, 101–108.

Bundi, A., & Wüthrich, K. (1979) *Biopolymers 18*, 285–297.

Dunn, D. (1981) *Trans. Am. Philos. Soc. 71*, 3–115.

Fogh, R. H., Mabbutt, B. C., Kem, W. R., & Norton, R. S. (1989) *Biochemistry* (following paper in this issue).

Gooley, P. R., & Norton, R. S. (1985) *Eur. J. Biochem. 153*, 529–539.

Gooley, P. R., & Norton, R. S. (1986a) *Biopolymers 25*, 489–506.

Gooley, P. R., & Norton, R. S. (1986b) *Biochemistry 25*, 2349–2356.

Gooley, P. R., Beress, L., & Norton, R. S. (1984a) *Biochemistry 23*, 2144–2152.

Gooley, P. R., Blunt, J. W., & Norton, R. S. (1984b) *FEBS Lett. 174*, 15–19.

Gooley, P. R., Blunt, J. W., Beress, L., Norton, T. R., & Norton, R. S. (1986) *J. Biol. Chem. 261*, 1536–1542.

Gooley, P. R., Blunt, J. W., Beress, L., & Norton, R. S. (1988) *Biopolymers 27*, 1143–1157.
Imoto, T., Johnson, L. N., North, A. C. T., Phillips, D. C., & Rupley, J. A. (1972) *Enzymes (3rd Ed.) 7*, 665–868.
Kaptein, R. (1982) in *Biological Magnetic Resonance* (Berliner, L., & Reuben, J., Eds.) Vol. 4, pp 145–191, Plenum Press, New York.
Kem, W. R. (1988) in *The Biology of Nematocysts* (Hessinger, D., & Lenhoff, H., Eds.) pp 375–405, Academic Press, New York.
Kem, W. R., Dunn, B. M., Parten, B. F., Pennington, M. W., & Price, D. (1986) *Fed. Proc., Fed. Am. Soc. Exp. Biol. 45*, 1795.
Metrione, R. M., Schweitz, H., & Walsh, K. A. (1987) *FEBS Lett. 218*, 59–62.
Norton, R. S., & Norton, T. R. (1979) *J. Biol. Chem. 254*, 10220–10226.
Norton, R. S., Zwick, J., & Beress, L. (1980) *Eur. J. Biochem. 113*, 75–83.
Norton, R. S., Norton, T. R., Sleigh, R. W., & Bishop, D. G. (1982) *Arch. Biochem. Biophys. 213*, 87–97.
Norton, R. S., Beress, L., Stob, S., Boelens, R., & Kaptein, R. (1986) *Eur. J. Biochem. 157*, 343–346.
Norton, T. R. (1981) *Fed. Proc., Fed. Am. Soc. Exp. Biol. 40*, 21–25.
Pennington, M. W., Kem, W. R., & Dunn, B. M. (1988) in *Macromolecular Sequencing and Analysis. Selected Methods and Applications* (Schlesinger, D. H., Ed.) pp 243–250, Liss, New York.
Schweitz, H., Vincent, J.-P., Barhanin, J., Frelin, C., Linden, G., Hugues, M., & Lazdunski, M. (1981) *Biochemistry 20*, 5245–5252.
Schweitz, H., Bidard, J.-N., Frelin, C., Pauron, D., Vijverberg, H. P. M., Mahasneh, D. M., Lazdunski, M., Vilbois, F., & Tsugita, M. (1985) *Biochemistry 24*, 3554–3561.
Torda, A. E., & Norton, R. S. (1987) *Biochem. Int. 15*, 659–666.
Torda, A. E., Mabbutt, B. C., van Gunsteren, W. F., & Norton, R. S. (1988) *FEBS Lett.* (in press).
Wagner, G., & Wüthrich, K. (1978) *Nature 275*, 247–248.
Wemmer, D. E., Kumar, N. V., Metrione, R. M., Lazdunski, M., Drobny, G., & Kallenbach, N. R. (1986) *Biochemistry 25*, 6842–6849.
Widmer, H., Wagner, G., Schweitz, H., Lazdunski, M., & Wüthrich, K. (1988) *Eur. J. Biochem. 171*, 177–192.
Wüthrich, K. (1986) *NMR of Proteins and Nucleic Acids*, Wiley, New York.
Zykova, T. A., Vinokurov, L. M., Kozlovskaya, E. P., & Elyakov, G. B. (1985) *Bioorg. Khim. 11*, 302–310.

Sequence-Specific ^{1}H NMR Assignments and Secondary Structure in the Sea Anemone Polypeptide *Stichodactyla helianthus* Neurotoxin I†

Rasmus H. Fogh,‡ Bridget C. Mabbutt,‡ William R. Kem,§ and Raymond S. Norton*,‡
School of Biochemistry, University of New South Wales, Kensington, New South Wales 2033, Australia, and Department of Pharmacology and Therapeutics, University of Florida, Gainesville, Florida 32610
Received August 3, 1988; Revised Manuscript Received September 21, 1988

ABSTRACT: Sequence-specific assignments are reported for the 500-MHz ^{1}H nuclear magnetic resonance (NMR) spectrum of the 48-residue polypeptide neurotoxin I from the sea anemone *Stichodactyla helianthus* (Sh I). Spin systems were first identified by using two-dimensional relayed or multiple quantum filtered correlation spectroscopy, double quantum spectroscopy, and spin lock experiments. Specific resonance assignments were then obtained from nuclear Overhauser enhancement (NOE) connectivities between protons from residues adjacent in the amino acid sequence. Of a total of 265 potentially observable resonances, 248 (i.e., 94%) were assigned, arising from 39 completely and 9 partially assigned amino acid spin systems. The secondary structure of Sh I was defined on the basis of the pattern of sequential NOE connectivities, NOEs between protons on separate strands of the polypeptide backbone, and backbone amide exchange rates. Sh I contains a four-stranded antiparallel β-sheet encompassing residues 1–5, 16–24, 30–33, and 40–46, with a β-bulge at residues 17 and 18 and a reverse turn, probably a type II β-turn, involving residues 27–30. No evidence of α-helical structure was found.

In the preceding paper (Norton et al., 1989) we presented the results of an investigation by ^{1}H NMR spectroscopy of the solution properties of the polypeptide neurotoxin I (Sh I)[1] from the Caribbean sea anemone *Stichodactyla helianthus*. This molecule is a representative of a new class of sea anemone polypeptides that are neurotoxic by virtue of their specific interaction with the nerve sodium channel (Kem, 1988). Other members of this class are *Heteractis* [formerly *Radianthus* (Dunn, 1981)] *macrodactylus* toxin III (Zykova et al., 1985)

† This work was supported in part by grants from the Australian Research Grants Scheme (R.S.N.) and the National Institutes of Health (Grant GM 32848 to W.R.K.). One of us (R.H.F.) thanks the Danish Medical Research Council and the Carlsberg Foundation for travel grants.
* Address correspondence to this author.
‡ University of New South Wales.
§ University of Florida.

[1] Abbreviations: Sh I, *Stichodactyla* (formerly *Stoichactis*) *helianthus* neurotoxin I; Hm III, *Heteractis* (formerly *Radianthus*) *macrodactylus* toxin III; Hp II and III, *Heteractis* (formerly *Radianthus*) *paumotensis* toxins II and III; AP-A, anthopleurin A; ATX I and II, *Anemonia sulcata* toxins I and II; 2D, two dimensional; DQF- (or TQF-) COSY, double (or triple) quantum filtered 2D homonuclear correlated spectroscopy; NOESY, 2D homonuclear nuclear Overhauser enhancement spectroscopy; RELAY, 2D homonuclear relayed coherence transfer spectroscopy; DQ, 2D homonuclear double quantum coherence spectroscopy; HOHAHA, 2D homonuclear Hartmann–Hahn spectroscopy; NOE, nuclear Overhauser enhancement; $d_{AB}(i,j)$, distance between proton type A and B located, respectively, in amino acid residues i and j; d_{AB}, the sequential connectivity $d_{AB}(i,i+1)$.

0006-2960/89/0428-1826$01.50/0